Ab Initio Based Configuration Interaction Calculations on the Low-Lying Electronic States of GaAs

Biswabrata Manna and Kalyan Kumar Das*

Department of Chemistry, Physical Chemistry Section, Jadavpur University, Calcutta 700 032, India

Received: April 17, 1998; In Final Form: July 31, 1998

Multireference singles and doubles configuration interaction calculations which include relativistic effective core potentials have been performed on GaAs. Potential energy curves of 40 Λ−S states are computed. Spectroscopic constants (T_e, r_e, and ω_e) of 17 bound Λ−S states have been estimated and compared with the available observed and other calculated values. The lowest Λ−S state is $...\pi^2\ X^3\Sigma^-$. All 22 Λ −S states which dissociate into $Ga(^2P_u) + As(^4S_u)$ and $Ga(^2P_u) + As(^2D_u)$ limits are taken into consideration for the spin−orbit CI calculations. Potential energy curves of 51 Ω-states are computed. The $X^3\Sigma^-_{0^+}$ component is found to be the ground state of GaAs in contrary to the experimental findings which suggest the other component $X^3\Sigma_1^-$ as the ground state. The splitting between the two components of $X^3\Sigma^-$ is calculated to be 76 cm^{-1} as compared with the experimental value of 43 cm^{-1}. The excited $A^3\Pi_{0^+}$ state, which does not predissociate has $r_e = 2.757$ Å, $T_e = 22\,178$ cm^{-1}, and $\omega_e = 125$ cm^{-1}. T_e and ω_e values are somewhat smaller, while r_e is larger than the observed data. Transition probabilities of several dipole allowed transitions are calculated. Three transitions such as $1^1\Sigma^+-4^1\Sigma^+$, $2^1\Sigma^+-4^1\Sigma^+$, and $X^3\Sigma^--A^3\Pi$ are found to be very strong. The radiative lifetimes of many excited states are also estimated. The $A^3\Pi_{0^+}$ state at the vibrational level $v' = 0$ has the calculated radiative lifetime of 1050 ns which is somewhat larger than the observed range.

I. Introduction

Over the past decade there has been considerable interest in the experimental and theoretical studies of mixed group III−V and other semiconductor clusters and small molecules. Especially, compounds such as GaP, InP, GaAs, InSb and their neutral and ionic clusters of different sizes are important materials because of their technological applications. Extensive studies on the clusters of GaAs with different sizes have been made by Smalley and co-workers.[1−5]

Historically, O'Brien et al.[1] have pioneered in generating the supersonic molecular beams of semiconductor clusters such as Ga_xAs_y by the laser vaporization of pure GaAs crystal mounted on the side of a pulsed supersonic nozzle. These cluster-beams are characterized by laser photoionization followed by time-of-flight mass spectrometry measurements. Liu et al.[2] have determined the electron affinities of GaAs, Si, and Ge clusters as a function of cluster size from the photodetachment and photofragmentation studies of these cluster anions. Photodissociations of the positive ions of these clusters are also studied.[3] Wang et al.[4] have studied the reactivity of NH_3 on the gallium arsenide cluster surface. Ultraviolet photoelectron spectra of mass-selected negative gallium arsenide cluster ions have been recorded by Jin et al.[5]

Although clusters of gallium arsenide have been studied extensively, Lemire et al.[6] are the first group who have studied the gas-phase diatomic GaAs molecules spectroscopically. The $^3\Pi-X^3\Sigma^-$ electronic band system which is located in the range 23 000−24 800 cm^{-1} has been observed in a resonant two-photon ionization study of the jet-cooled GaAs molecule. The upper state, which is the third $^3\Pi$ state, has been found to correlate with the $Ga(^2P_u) + As(^2D_u)$ dissociation limit. This $^3\Pi-X^3\Sigma^-$ band system is found to be useful in probing the reaction mechanism of organometallic vapor phase epitaxial growth of GaAs films on suitable substrates which provide a means for the production of electronic devices. High-resolution spectra of the $^3\Pi-X^3\Sigma^-$ band taken by Lemire et al.[6] have revealed that there occurs a predissociation of the $^3\Pi$ state for $v' \geq 1$ for $\Omega = 2, 1, 0^-$ components while the 0^+ component survives. It is proposed that 2, 1, and 0^- components of the repulsive $1^5\Sigma^-$ state are coupled with the components of $^3\Pi$ to induce the predissociation of the excited $^3\Pi$ state. The lifetimes for individual vibronic levels of the excited $^3\Pi$ state have been measured and found to be widely fluctuating ranging from $\tau =$ 600 ns ($v' = 0$, $\Omega' = 0^+$) to $\tau = 10$ ns ($v' = 1$, $\Omega' = 2$). The bond strength estimated from this experiment is found to be D_o (GaAs) = 2.06 ± 0.05 eV. Small gallium arsenide clusters are also studied by Van Zee et al.[7] by using matrix-isolated ESR spectroscopy. Knight and Petty[8] have observed ESR spectra of $GaAs^+$ from the laser vaporization and photoionization of GaAs.

Because of the technological applications of GaAs as a semiconducting material, several theoretical studies[9−11] have been carried out for its bulk properties. Ab initio based CASSCF/CI calculations have been performed by Balasubramanian[12−14] on GaAs, $GaAs^+$, and $GaAs^-$ molecules. Meier et al.[15] have carried out MRDCI calculations on GaAs and $GaAs^+$ to compute potential energy curves and spectroscopic constants of several low-lying electronic states. However, none of these calculations include the spin−orbit interaction in the Hamiltonian. The transition probability of the observed transition $^3\Pi-X^3\Sigma^-$ has not been calculated as yet. The electronic and geometrical structure of small Ga_xAs_y clusters in stoichiometric and nonstoichiometric compositions have been calculated by using local spin density method.[16,17] These calculations show

* Author for correspondence.

10.1021/jp981902d CCC: $15.00
Published on Web 11/10/1998

that even numbered clusters tend to be singlets, while odd numbered belong to higher multiplets.

The present paper deals with the computation of the potential energy curves and spectroscopic properties of many low-lying electronic states without and with spin−orbit coupling by using ab initio based multireference singles and doubles configuration interaction (MRDCI) method which takes care of the relativistic effects through the effective core potential. We have focused our attention on several dipole allowed transitions. The transition probabilities of these radiative transitions are calculated, and lifetimes of the upper states are also estimated and compared with observed data.

II. Method of Computations

Relativistic effective core potentials (RECP) of the semicore type for both gallium and arsenic atoms are taken from Hurley et al.[18] The $3d^{10}4s^24p$ and $3d^{10}4s^24p^3$ electrons for Ga and As, respectively, are being kept in the valence space, while the remaining inner electrons are replaced by RECPs. As a result, the number of active electrons for GaAs has been reduced to 28. The Gaussian basis sets chosen for the present calculations are of the type (3s3p4d/3s3p3d) which are optimized by Hurley et al.[18] themselves. We have performed a self-consistent-field (SCF) calculation for a repulsive $1^5\Sigma^-$ state with 28 valence electrons at each internuclear separation of the potential energy curve. The optimized SCF-MOs generated are used as one electron functions for the configuration interaction (CI) calculations. Preliminary calculations reveal that 20 electrons occupying 3d shells of Ga and As do not participate actively in forming the Ga−As bond in the low-lying excited states. We have, therefore, kept these d-electrons frozen in CI steps. Hence only eight electrons remain active in the CI space. The MRDCI method of Buenker and co-workers[19−22] has been employed for the calculation of the ground and low-lying excited Λ −S states without the spin−orbit interaction but with the inclusion of all spin independent relativistic effects by using RECPs. The CI codes of Buenker and co-workers[19−22] have been used for the present calculations. The codes take care of different open shell configurations efficiently by using the Table CI algorithm.[23,24] For simplicity, the present calculations have been performed in the C_{2v} subgroup of $C_{\infty v}$. A set of main reference configurations is chosen for the lowest eight roots of each irreducible representation of a given spin multiplicity to describe low-lying excited states. All single and double excitations have been carried out from these reference configurations. The configuration selection and energy extrapolation technique along with the Davidson correction[25,26] are used to estimate the full CI energy in the same AO basis. The threshold value for the configuration selection is chosen as 2μ hartree throughout the calculation. The dimensions of the secular equations corresponding to the generated CI space are of the order of 400 000, while for the selected configuration space it is around 10 000. The CI wave functions obtained from these calculations are used to compute the one electron property matrix elements.

The spin−orbit calculations are carried out in the C_{2v}^2 group. The spin−orbit operators which are derived from RECPs of Ga and As are taken from Hurley et al.[18] The eigenfunctions obtained from the spin independent CI are multiplied with appropriate spin functions which transform as C_{2v} irreducible representations. The estimated full CI energies obtained in Λ−S CI calculations are kept as diagonal Hamiltonian matrix elements, while the off-diagonal elements are computed by using the RECP spin-operators and Λ−S CI wave functions. The Wigner-Eckart theorem is used to compute final results.[27] All spin components of the Λ−S eigenfunctions obtained from the above spin-independent calculations are included in the spin−orbit treatment. For the even electron GaAs molecule, singlet, triplet, and quintet states of each symmetry are taken into consideration. A_1, A_2, and B_1 representations consist of all spin−orbit states. Many-electron spin−orbit matrix elements for pairs of M_s values are computed. The spin−orbit CI wave functions are then used for getting the transition properties.

Both Λ−S and Ω potential energy curves are fitted into polynomials, and vibrational Schrödinger equations are solved numerically.[28] The electric transition dipole moments are averaged over pairs of vibrational functions involved in a given electronic transition. Transition probabilities of different dipole allowed transitions are computed. The radiative lifetimes of excited vibrational levels are obtained from their respective transition probabilities.

TABLE 1: Dissociation Correlation between the Atomic States and the Molecular States of GaAs without Including the Spin−Orbit Coupling

molecular states (Λ−S)	atomic states in the dissociation limits	relative energies (in cm^{-1}) expt[a]	relative energies (in cm^{-1}) calculation
$^3\Sigma^-$, $^3\Pi$, $^5\Sigma^-$, $^5\Pi$	$^2P_u(Ga) + {}^4S_u(As)$	0	0
$^1\Sigma^+$, $^1\Sigma^-(2)$, $^1\Pi(3)$, $^1\Delta(2)$, $^1\Phi$, $^3\Sigma^+$, $^3\Sigma^-(2)$, $^3\Pi(3)$, $^3\Delta(2)$, $^3\Phi$	$^2P_u(Ga) + {}^2D_u(As)$	10790	14353
$^1\Sigma^+(2)$, $^1\Sigma^-$, $^1\Pi(2)$, $^1\Delta$, $^3\Sigma^+(2)$, $^3\Sigma^-$, $^3\Pi(2)$, $^3\Delta$	$^2P_u(Ga) + {}^2P_u(As)$	18530	19774

[a] Moore's table [ref 29]; energies are averaged over j.

III. Computed Results and Discussion

Potential Energy Curves and Composition of Λ−S States. The ground state (^2P_u) of Ga combines with the ground state (^4S_u) of As to generate four states of triplet and quintet multiplicities: $^3\Sigma^-$, $^3\Pi$, $^5\Sigma^-$, and $^5\Pi$. However, the combination of the ground state of Ga with the low-lying ^2D_u and ^2P_u excited states of As results a large number of molecular states of the singlet and triplet multiplicities. Table 1 shows the dissociation relationship between the atomic states and the molecular states of GaAs in the absence of any spin−orbit mixing. We have compared the relative energies at the dissociation limits calculated in this work with the experimental data[29] averaged over j. The computed energies are found to be larger than the observed data by 1200−3500 cm^{-1}. In the present study we have considered all possible 34 Λ−S states which dissociate into $Ga(^2P_u) + As(^4S_u)$, $Ga(^2P_u) + As(^2D_u)$, and $Ga(^2P_u) + As(^2P_u)$ limits and six other states which correlate with still higher dissociation limits. In Figure 1a, we have plotted the computed potential energy curves of all triplet and quintet Λ−S states of GaAs, while singlet curves are drawn in Figure 1b. The corresponding electronic energy differences (T_e), equilibrium bond distances (r_e), and vibrational frequencies (ω_e) of 17 bound Λ−S states of GaAs are given in Table 2. The remaining 23 Λ−S states are repulsive in nature. The ground state of GaAs is $X^3\Sigma^-$ with an open shell configuration. The calculated equilibrium bond length is about 0.14 Å larger than the observed r_e. However, the vibrational frequency is about 36 cm^{-1} smaller. The ground-state wave function is dominated by the open shell configuration $...\pi^2$ which generates two more states: $1^1\Delta$ and $2^1\Sigma^+$. Both of these states are very strongly bound. The $1^1\Delta$ state is lying fifth in the energy ordering with $T_e = 8498$ cm^{-1}. In addition to $...\pi^2$, 3% of the$...\pi\pi$ configuration contributes in the $1^1\Delta$ state. The r_e and ω_e of $1^1\Delta$ are comparable with those of the ground state. The $2^1\Sigma^+$ state which is next to $1^1\Delta$ is

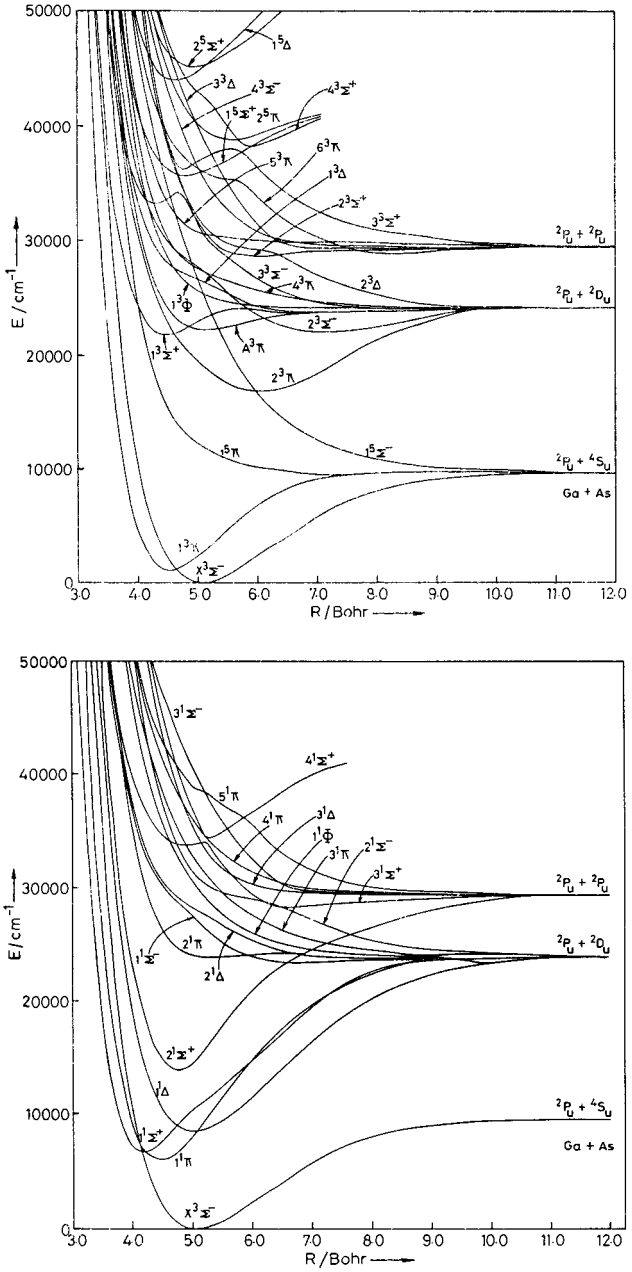

Figure 1. (a) Potential energy curves of triplet and quintet Λ−S states of GaAs. (b) Potential energy curves of singlet Λ−S states of GaAs.

lying 13 956 cm^{-1} above the ground state. Two more configurations: $...\pi^4$ and $...\pi^3\pi$ contribute significantly to the description of the $2^1\Sigma^+$ state. The Ga−As bond in the $2^1\Sigma^+$ state is found to be relatively strong with $r_e = 2.515$ Å and $\omega_e = 269$ cm^{-1}. The $X^3\Sigma^-$, $1^1\Delta$, and $2^1\Sigma^+$ states dissociate into three different limits in the increasing order.

The lowest excited $1^3\Pi$ state arises from a single excitation $\sigma_3^2\pi^2 \rightarrow \sigma_3\pi^3$ which also generates the corresponding singlet counterpart. The $1^3\Pi$ state is only 1066 cm^{-1} above the ground state, while the transition energy of $1^1\Pi$ is about 5941 cm^{-1}. The equilibrium bond lengths of both $1^3\Pi$ and $1^1\Pi$ are comparatively shorter than the ground-state r_e. The vibrational frequencies of these two states are in the range 235−270 cm^{-1}. The $1^3\Pi$ state correlates with $Ga(^2P_u) + As(^4S_u)$, while the $1^1\Pi$ state dissociates into the upper limit $Ga(^2P_u) + As(^2D_u)$. Besides $...\sigma_3\pi^3$, there exists one more configuration $...\sigma_3\pi^2\pi$ which contributes significantly to both the low-lying Π states. The fourth Λ−S state of GaAs is a stable $1^1\Sigma^+$ state which is dominated by a closed-shell configuration $...\pi^4$ ($c^2 = 0.52$) and three open shell configurations: $...\pi^3\pi$ ($c^2 = 0.28$), $...\sigma_2\sigma_3\pi^4$ ($c^2 = 0.06$), and $...\pi^2$ ($c^2 = 0.02$). The $1^1\Sigma^+$ state has the shortest bond length ($r_e = 2.21$ Å) and comparatively large vibrational frequency ($\omega_e = 294$ cm^{-1}), and it dissociates into the second asymptote $Ga(^2P_u) + As(^2D_u)$.

The $2^3\Pi$ state is relatively weakly bound with a broad and shallow potential well. Single excitations of the type $\sigma \rightarrow \pi^*$ and $\sigma \rightarrow \pi$ from the ground-state configuration $...\sigma^2\pi^2$ dominate in the formation of the $2^3\Pi$ state. It is noted that the $1^3\Pi$ state is predominantly $...\sigma_3\pi^3$. The $...\sigma\pi^2\pi$ configuration gives rise to 10 Λ−S states: $^1\Pi$ (3), $^1\Phi$, $^3\Pi_r$ (2), $^3\Pi_i$ (2), $^3\Phi$, and $^5\Pi$. Of these, both $1^1\Phi$ and $1^3\Phi$ states are repulsive in nature and they dissociate into the second asymptote, while the repulsive $1^5\Pi$ state correlates with the ground dissociation limit. Among three $^1\Pi$ states originating from $...\sigma\pi^2\pi$, only $2^1\Pi$ is very weakly bound with $\omega_e = 98$ cm^{-1}, while $3^1\Pi$ and $4^1\Pi$ are repulsive. The third $^3\Pi$ state which is designated here as $A^3\Pi$ has a special importance because of the observed $A^3\Pi-X^3\Sigma^-$ band system.[6] The remaining two $^3\Pi$ states, namely, $4^3\Pi$ and $5^3\Pi$, are repulsive. Analyzing the CI wave functions it has been found that the $A^3\Pi$ state has about 81% character of the $...\sigma_3\pi^2\pi$ configuration. The computed transition energy of $A^3\Pi$ is 22 250 cm^{-1} which matches well with the observed average T_e of 23 545 cm^{-1}. The observed r_e and ω_e values reported in Table 2 are for the 0^+ component of $A^3\Pi$ for which other Ω components are found to predissociate. Thus the inclusion of the spin−orbit interaction is desired for the meaningful comparison with the observed data. We shall return to this aspect in the next section where we discuss the effect of the spin−orbit coupling.

There is a strongly bound $1^3\Sigma^+$ state with a T_e value of 21 852 cm^{-1}. This state arises mainly from the closed-shell $1^1\Sigma^+$ state through a single excitation $\pi^4 \rightarrow \pi^3\pi^*$. However, several other multiple excitations also occur with smaller contributions. The $2^3\Sigma^-$ state has a very shallow potential well with much longer bond length. Figure 1a shows an avoided crossing of this state with its next higher repulsive state $3^3\Sigma^-$ at around 5.3a_o. Both these states dissociate into the second asymptote. The $2^3\Sigma^+$ state comes next in the energy ordering. It is seen from the adiabatic curve in Figure 1a that the $2^3\Sigma^+$ curve undergoes strong avoided crossings with the weakly bound and repulsive potential energy curves of $3^3\Sigma^+$ and $4^3\Sigma^+$ at around 4.7a_o and 5.7a_o, respectively. As a result the adiabatic curve of the $2^3\Sigma^+$ state shows a double minima. The minimum appearing at the long distance is very shallow. The minimum at the shorter distance ($r_e = 2.263$ Å) lying 33 270 cm^{-1} above the ground state is very deep and its composition at r_e is found to be a mixture of $...\sigma_2\sigma_3\pi^4$ ($c^2 = 0.4$), $...\sigma_2\sigma_3\pi^3\pi$ ($c^2 = 0.27$), and $...\sigma_2^2\pi^3\pi$ ($c^2 = 0.19$). The computed CI wave functions show similar mixing for the $3^3\Sigma^+$ state at $r = 5.2a_o$ and for the $4^3\Sigma^+$ state at $r = 6.5a_o$. This essentially confirms strong avoided crossings among these states. However, the fitted potential well of $2^3\Sigma^+$ with shorter r_e contains only three vibrational levels.

A strongly bound excited $4^1\Sigma^+$ state has been obtained at 33 776 cm^{-1} of energy in our calculations. This state has a minimum at 2.586 Å with $\omega_e = 172$ cm^{-1}. A sharp avoided crossing at 5.2a_o between the bound $4^1\Sigma^+$ state and a repulsive $3^1\Sigma^+$ state is seen in Figure 1b. The diabatic potential energy curve of the $4^1\Sigma^+$ state dissociates into the higher asymptote. At around the equilibrium bond length, the $4^1\Sigma^+$ state shows complicated character, and six configurations interact strongly. However, to adequately describe so highly excited states

TABLE 2: Spectroscopic Parameters of the Bound Λ−S States of GaAs

state	T_e (cm^{-1})	r_e (Å)	ω_e (cm^{-1})
$X^3\Sigma^-$	0	2.670 (2.60)[b] [2.53][a]	179 (215)[b] [215][a]
$1^3\Pi$	1066 (1830)[b]	2.398 (2.38)[b]	236 (236)[b]
$1^1\Pi$	5941 (6440)[b]	2.356 (2.34)[b]	270 (277)[b]
$1^1\Sigma^+$	6690 (7768)[b]	2.210 (2.23)[b]	294 (279)[b]
$1^1\Delta$	8498 (7874)[b]	2.651 (2.58)[b]	193 (214)[b]
$2^1\Sigma^+$	13956 (14383)[b]	2.515 (2.47)[b]	269 (321)[b]
$2^3\Pi$	16832 (18590)[b] (17700)[d]	3.207 (3.10)[b] (3.21)[d]	126 (135)[b] (132)[d]
$1^3\Sigma^+$	21852 (23403)[b]	2.374 (2.405)[b]	209 (208)[b]
$2^3\Sigma^-$	22020	3.766	85
$A^3\Pi$	22250 (24600)[b] (21600)[d] [23545][a]	2.717 (2.68)[b] (2.70)[d] [2.662][a]	135 (160)[b] (150)[d] [152][a]
$2^1\Pi$	23953 (24679)[c]	2.789 (2.693)[c]	98 (148)[c]
$2^3\Sigma^+$	33270 (31106)[c]	2.263 (2.421)[c]	298 (201)[c]
$4^1\Sigma^+$	33776	2.586	172
$1^5\Sigma^+$	35717	2.546	178
$2^5\Pi$	38843 (40352)[c]	2.957 (2.818)[c]	138 (168)[c]
$1^5\Delta$	43986 (45431)[c]	2.460 (2.449)[c]	223 (287)[c]
$2^5\Sigma^+$	45157	2.616	196

[a] Experimental values [ref 6]. [b] CASSCF/SOCI calculated results [ref 14]. [c] CASSCF/FOCI calculated results [ref 14]. [d] Other calculated results [ref 15].

especially, near the dissociation limit, it would be necessary to use Rydberg functions.[15]

Among the quintet states studied here, $1^5\Pi$ and $1^5\Sigma^-$ are repulsive and dissociate into the ground atomic states Ga(^2P_u) + As(^4S_u). The $1^5\Pi$ state is mainly dominated by the $...\sigma_3\pi^2\pi$ configuration, while the $1^5\Sigma^-$ state is characterized by the $...\sigma_3\sigma_4\pi^2$ ($c^2 = 0.88$) configuration. The remaining four quintet states of GaAs, $1^5\Sigma^+$, $2^5\Pi$, $1^5\Delta$, and $2^5\Sigma^+$, are high-lying but strongly bound (see Figure 1a). The $1^5\Sigma^+$ and $2^5\Sigma^+$ states are separated by about 9440 cm^{-1}. The $1^5\Sigma^+$ state has a shorter bond length ($r_e = 2.546$ Å) than $2^5\Sigma^+$ ($r_e = 2.616$ Å), while the vibrational frequency of the former state is lower by about 20 cm^{-1} (see Table 2). Three configurations: $...\sigma_2\sigma_3\pi^3\pi$, $...\sigma_2^2\pi^2\pi^2$, and $...\sigma_2\sigma_3\pi^2\pi^2$ contribute significantly in the characterization of both these states. Of the remaining two quintet states, $1^5\Delta$ is lying 43 986 cm^{-1} above the ground state, and it has a shorter r_e (2.46 Å) with $\omega_e = 223$ cm^{-1}. This state has almost a pure character of $...\sigma_2\sigma_3\pi^3\pi$ ($c^2 = 0.92$). The $2^5\Pi$ state which is characterized dominantly by the $...\sigma_2\sigma_3^2\pi^2\pi$ configuration has a longer r_e and smaller ω_e. These highly excited quintet states require Rydberg functions in the basis set for their adequate description.[15] The present calculations do not include any Rydberg functions, and hence these quintets may not be very accurate.

The ground-state dissociation energy of GaAs estimated from the MRDCI calculation has been found to be 1.3 eV which is much lower than the value 2.06 ± 0.05 eV obtained from the experimental data.[6] The present value is comparable with the CASSCF/FOCI D_e value.[14] Meier [15] has shown an improvement of about 0.2 eV due to the d-correlation. The extension of the basis set would also improve the D_e value as predicted by Balasubramanian.[14]

Effects of the Spin−Orbit Coupling. Spin−orbit coupling is introduced through the inclusion of the spin−orbit operator[18] derived from RECPs. As a result Λ−S states of different symmetries interact through the same Ω-components. In Table 3, we have given the dissociation correlation between the molecular Ω states and the atomic states in the presence of the spin−orbit interaction. Here in this study we have considered only those Λ−S states which dissociate into the lowest two asymptotes: ^2P_u(Ga) + ^4S_u(As) and ^2P_u(Ga) + ^2D_u(As). In otherwords, we have included 22 Λ−S states in the spin−orbit CI calculations. Due to the spin−orbit coupling, two dissociation limits split into six asymptotes. Relative energies of these asymptotes are compared with the experimental data.[29] The computed energies are somewhat larger than the observed data except for the lowest two limits for which the agreement is good.

TABLE 3: Dissociation Correlation between the Atomic States and the Molecular States of GaAs with the Inclusion of the Spin−Orbit Coupling

molecular states (Ω)	atomic states in the dissociation limits Ga + As	relative energies (in cm^{-1}) expt.[a]	calculation
$2,1,1,0^+,0^-$	$^2P_{1/2} + {}^4S_{3/2}$	0	0
$3,2,2,1,1,1,0^+,0^+,0^-,0^-$	$^2P_{3/2} + {}^4S_{3/2}$	826	735
$2,1,1,0^+,0^-$	$^2P_{1/2} + {}^2D_{3/2}$	10593	14129
$3,2,2,1,1,0^+,0^-$	$^2P_{1/2} + {}^2D_{5/2}$	10915	14526
$3,2,2,1,1,1,0^+,0^+,0^-,0^-$	$^2P_{3/2} + {}^2D_{3/2}$	11419	14884
$4,3,3,2,2,2,1,1,1,1,0^+,0^+,0^-,0^-$	$^2P_{3/2} + {}^2D_{5/2}$	11741	15266

[a] Moore's table [ref 29].

There are 51 spin−orbit states with $\Omega = 0^+$, 0^-, 1, 2, 3, and 4 generated from 22 Λ−S states. In Figure 2, potential energy curves of nine states with $\Omega = 0^+$ are plotted. The $X^3\Sigma^-_{0^+}$ component dissociates into Ga($^2P_{1/2}$) + As($^4S_{3/2}$) while the $1^3\Pi_{0^+}$ and $1^5\Pi_{0^+}$ components correlate with Ga($^2P_{3/2}$) + As($^4S_{3/2}$). Several sharp avoided crossings are noted in Figure 2. Potential energy curves of all nine states of the 0^- symmetry are shown in Figure 3. The 0^- component of $1^3\Pi$ correlates with the lowest asymptote. We have plotted potential energies of the states with $\Omega = 2$ and 4 in Figure 4. The remaining 16 states with $\Omega = 1$ and two states with $\Omega = 3$ are drawn in Figure 5. We have left out three repulsive states with $\Omega = 3$ to avoid further complicacy in Figure 5. Spectroscopic constants of 18 low-lying Ω states below 23 000 cm^{-1} are reported in Table 3.

The ground state splits into two components: $X^3\Sigma^-_{0^+}$ and $X^3\Sigma_1^-$. The present calculations predict the $X^3\Sigma^-_{0^+}$ component to be lower than the other by about 76 cm^{-1}. However, high-resolution spectroscopic experiments on jet-cooled GaAs by Lemire et al.[6] have shown the opposite trend. The $X^3\Sigma_1^-$ state has been identified as the ground state with the $X^3\Sigma^-_{0^+}$ substate lying 43 cm^{-1} above it. The CI estimated equilibrium bond lengths of both components of the $X^3\Sigma^-$ state are about 0.12 Å longer than the observed values. The corresponding calculated ω_e values are smaller than the experimental results by about 30 cm^{-1}. Four components of the $1^3\Pi$ state are separated at the

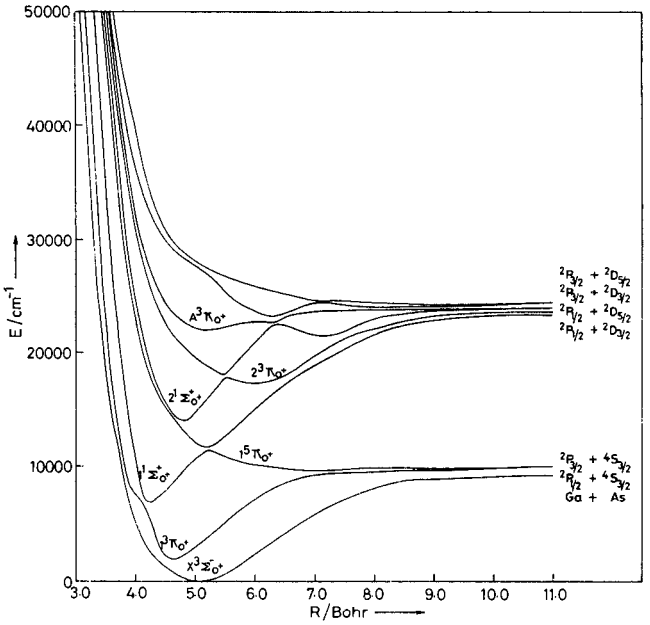

Figure 2. Potential energy curves of low-lying $\Omega = 0^+$ states of GaAs.

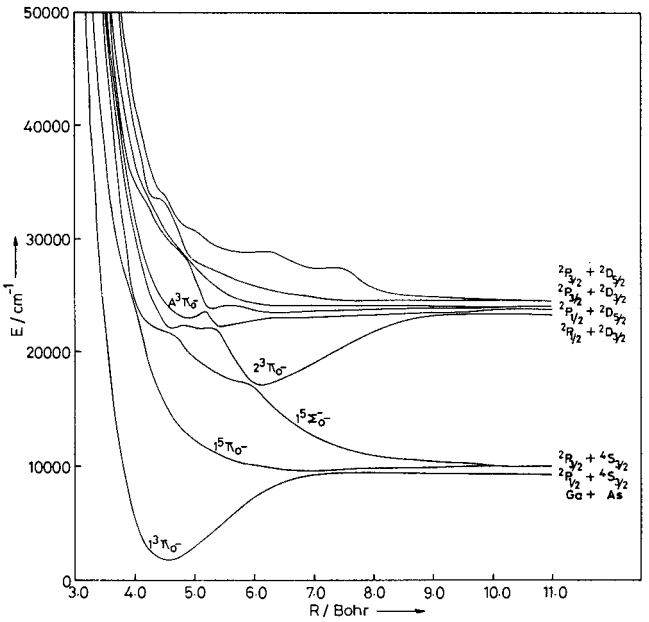

Figure 3. Potential energy curves of low-lying $\Omega = 0^-$ states of GaAs.

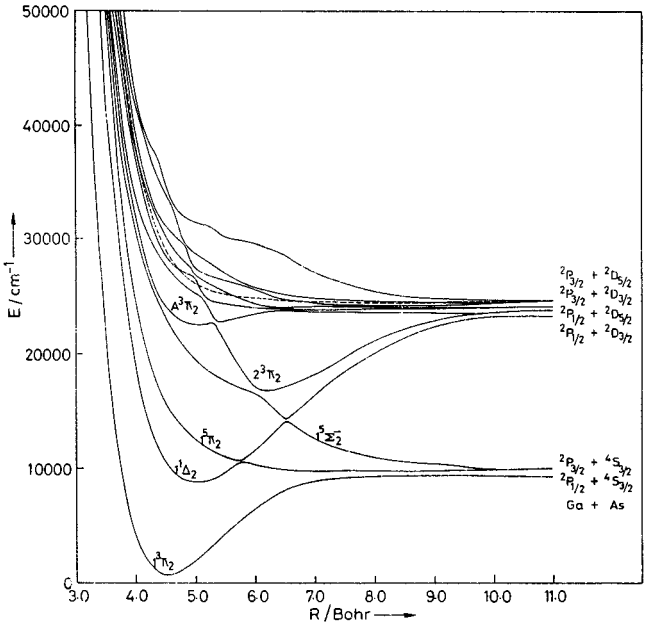

Figure 4. Potential energy curves of low-lying $\Omega = 2$ and 4 states of GaAs (the curve with dashed line is for $\Omega = 4$).

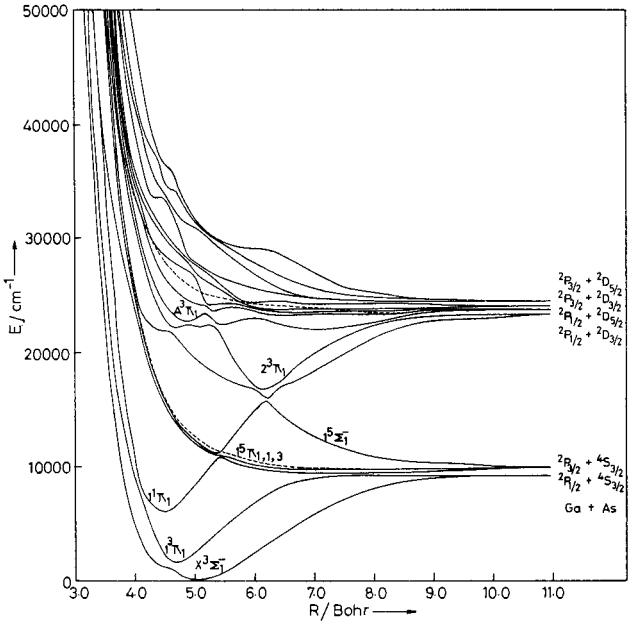

Figure 5. Potential energy curves of low-lying $\Omega = 1$ and 3 states of GaAs (curves with dashed lines are for $\Omega = 3$).

most by about 1050 cm^{-1}. The $1^3\Pi_2$ and $1^3\Pi_{0^-}$ substates do not have any nearby components of the same symmetries for mixing. As a result, these two components remain almost pure $1^3\Pi$ (see Table 4). Two other components $1^3\Pi_{0^+}$ and $1^3\Pi_1$ interact with $X^3\Sigma^-_{0^+}$ and $X^3\Sigma^-_1$, respectively. As seen from Table 4, about 67% $1^3\Pi$ and 30% $1^3\Sigma^-$ contribute to the $1^3\Pi_{0^+}$ state at r_e. Multiple avoided crossings are also evident from Figures 2 and 5. The $1^1\Pi_1$ component is not affected much by the spin−orbit coupling. Its T_e value is increased by 350 cm^{-1}. A similar situation has been noted for three successive singlet states: $1^1\Sigma^+_{0^+}$, $1^1\Delta_2$, and $2^1\Sigma^+_{0^+}$. The energies of the four components of the next important $2^3\Pi$ state are 2, 1, 0^+, and 0^- in the ascending order. Although these Ω-states undergo avoided crossing, we have fitted the diabatic potential energy curves for spectroscopic parameters listed in Table 4. Three components $\Omega = 2$, 1, and 0^- of the repulsive $1^5\Sigma^-$ state undergo avoided crossings with the same components of the $2^3\Pi$ state. Both the components of the $1^3\Sigma^+$ state show multiple crossings within a small range of bond distance in the potential energy curves. We could not fit the diabatic potential energies of the $1^3\Sigma^+_{0^-}$ and $1^3\Sigma^+_1$ components. The adiabatic curves are found to be predissociating. However, there are no experimental evidences for these states.

The third $^3\Pi$ state which we designate as $A^3\Pi$ is spectroscopically observed. The $A^3\Pi-X^3\Sigma^-$ band system in the jet-cooled GaAs molecule has been studied in detail.[6] The present spin−orbit CI calculations reveal four components $A^3\Sigma_{0^-}$, $A^3\Pi_{0^+}$, $A^3\Pi_1$, and $A^3\Pi_2$ in the same energy ordering as the experimental results. Transition energies of these components compare well with the observed values. Table 4 shows that the composition of these Ω-states is mainly $A^3\Pi$. Figure 2 shows that the $A^3\Pi_{0^+}$ component survives the predissociation, while the remaining three components $A^3\Pi_{0^-}$, $A^3\Pi_1$, and $A^3\Pi_2$ predissociate mainly due to their interactions with the corre-

TABLE 4: Spectroscopic Parameters of Low-Lying Spin−Orbit States of GaAs[a]

state	T_e (cm^{-1})	r_e (Å)	ω_e (cm^{-1})	dominant Λ−S states at r_e[b]
$X^3\Sigma^-_{0^+}$	0 [43]	2.673 [2.55]	180 [209]	$X^3\Sigma^-$ (97)
$X^3\Sigma^-_1$	76 [0]	2.667 [2.53]	181 [215]	$X^3\Sigma^-$ (97), $1^3\Pi$ (2.1)
$1^3\Pi_2$	736	2.396	234	$1^3\Pi$ (99.8)
$1^3\Pi_1$	1215	2.388	240	$1^3\Pi$ (97), $1^3\Sigma^-$ (2.3)
$1^3\Pi_{0^+}$	1751	2.389	234	$1^3\Pi$ (67), $1^3\Sigma^-$ (30.2)
$1^3\Pi_{0^-}$	1783	2.401	231	$1^3\Pi$ (99.8)
$1^1\Pi_1$	6283	2.356	265	$1^1\Pi$ (98)
$1^1\Sigma^+_{0^+}$	6947	2.218	297	$1^1\Sigma^+$ (99)
$1^1\Delta_2$	8771	2.649	189	$1^1\Delta$ (99)
$2^1\Sigma^+_{0^+}$	14231	2.523	270	$2^1\Sigma^+$ (99)
$2^3\Pi_2$	16794	3.218	122	$2^3\Pi$ (79), $1^5\Sigma^-$ (19.5)
$2^3\Pi_1$	17047	3.200	120	$2^3\Pi$ (56), $1^5\Sigma^-$ (41.6)
$2^3\Pi_{0^-}$	17203	3.172	128	$2^3\Pi$ (83.6), $2^5\Sigma^-$ (14.7)
$2^3\Pi_{0^+}$	17327	3.176	135	$2^3\Pi$ (98)
$A^3\Pi_{0^-}$	22142 [23545]	2.730	143	$A^3\Pi$ (98)
$A^3\Pi_{0^+}$	22178 [23568]	2.757 [2.662]	125 [152]	$A^3\Pi$ (99)
$A^3\Pi_1$	22265 [23760]	2.716	145	$A^3\Pi$ (94), $2^1\Pi$ (5)
$A^3\Pi_2$	22650 [24079]	2.694	135	$A^3\Pi$ (99)

[a] Values in square brackets represent the experimental values [ref 6]. [b] Values in parentheses are percentage contributions.

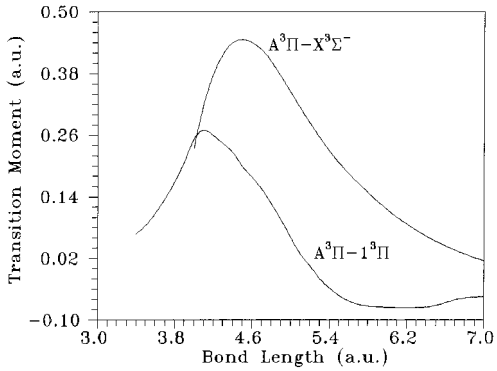

Figure 6. Transition dipole moment functions for $A^3\Pi-X^3\Sigma^-$ and $A^3\Pi-1^3\Pi$ transitions.

sponding Ω-components of the repulsive $1^5\Sigma^-$ state as evident from Figures 2−5. This feature confirms the experimental findings of Lemire et al.[6]

Transition Moments, Transition Probabilities, and Radiative Lifetimes. Experimentally,[6] vibronic bands of the $A^3\Pi-X^3\Sigma^-$ system of GaAs have been studied by using high-resolution spectroscopic measurement. The measured lifetimes of individual vibronic levels of the $A^3\Pi$ excited state of GaAs fluctuate very widely as functions of v', Ω', and isotopic composition. It falls in the range 600 ns−10 ns. In the present study we have calculated transition probabilities of several transitions which are allowed in Hund's case (a). In addition, we have also considered all possible transitions of type 0^+-0^+ and 0^+-1 which become allowed in case (c).

Figure 6 shows transition dipole moments of two important transitions $A^3\Pi-X^3\Sigma^-$ and $A^3\Pi-1^3\Pi$ as a function of the internuclear distance. Both the functions are smooth having maxima. The transition moment of the former transition is generally higher than that of the later. The transition dipole moments of 0^+-0^+ and 0^+-1 type transitions with the upper state being the component of $A^3\Pi$ are plotted in Figures 7 and 8, respectively. There are four allowed 0^+-0^+ transitions, namely, $A^3\Pi_{0^+}-1^3\Pi_{0^+}$, $A^3\Pi_{0^+}-1^1\Sigma^+_{0^+}$, $A^3\Pi_{0^+}-X^3\Sigma^-_{0^+}$, and $A^3\Pi_{0^+}-2^1\Sigma^+_{0^+}$, while three perpendicular 0^+-1 transitions ($\Delta\Omega = \pm1$) are $A^3\Pi_{0^+}-X^3\Sigma^-_1$, $A^3\Pi_{0^+}-1^3\Pi_1$, and $A^3\Pi_{0^+}-1^1\Pi_1$. We have estimated the transition probabilities from the

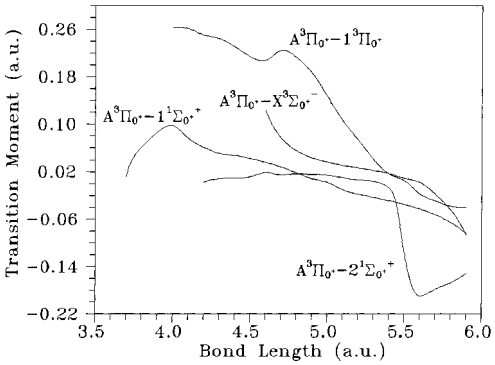

Figure 7. Transition dipole moment functions for 0^+-0^+ transitions of the $A^3\Pi_{0^+}$ state.

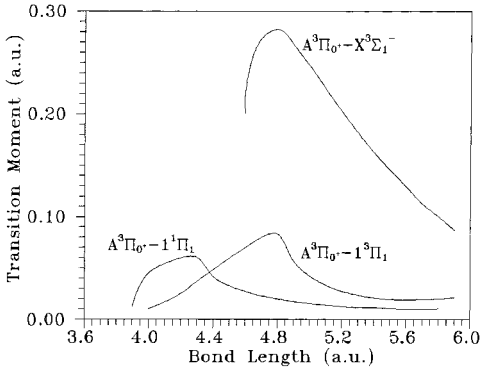

Figure 8. Transition dipole moment functions for 0^+-1 transitions of the $A^3\Pi_{0^+}$ state.

TABLE 5: Radiative Lifetimes of Some Excited Λ−S States ($v' = 0$) of GaAs

transition	partial lifetime of the upper state at $v' = 0$ (in sec)	total lifetime of the upper state at $v' = 0$ (in sec)
$1^1\Pi \leftarrow 2^1\Sigma^+$	8.04×10^{-6}	
$1^1\Sigma^+ \leftarrow 2^1\Sigma^+$	46.8×10^{-6}	$\tau(2^1\Sigma^+) = 6.9 \times 10^{-6}$
$1^3\Pi \leftarrow 1^3\Sigma^+$	1.3×10^{-6}	$\tau(1^3\Sigma^+) = 1.3 \times 10^{-6}$
$1^1\Sigma^+ \leftarrow 4^1\Sigma^+$	48.3×10^{-9}	
$2^1\Sigma^+ \leftarrow 4^1\Sigma^+$	396.5×10^{-9}	
$1^1\Pi \leftarrow 4^1\Sigma^+$	6.8×10^{-4}	$\tau(4^1\Sigma^+) = 43.1 \times 10^{-9}$
$X^3\Sigma^- \leftarrow 2^3\Pi$	82.8×10^{-6}	
$1^3\Pi \leftarrow 2^3\Pi$	1.3×10^{-1}	$\tau(2^3\Pi) = 82.7 \times 10^{-6}$
$X^3\Sigma^- \leftarrow A^3\Pi$	456×10^{-9}	
$1^3\Pi \leftarrow A^3\Pi$	14.8×10^{-6}	$\tau(A^3\Pi) = 440 \times 10^{-9}$
$1^3\Sigma^+ \leftarrow 2^3\Sigma^+$	19.1×10^{-6}	
$1^3\Pi \leftarrow 2^3\Sigma^+$	2.5×10^{-6}	$\tau(2^3\Sigma^+) = 2.2 \times 10^{-6}$

Einstein spontaneous emission coeffecients $A_{v'v''}$ (s^{-1}) between various vibrational levels v' of the upper electronic state and v'' level of the lower state. The calculations desire the knowledge of the electronic transition moment function which are taken from the curves shown in Figures 6−8. The radiative lifetimes are basically the reciprocal of the sum of $A_{v'v''}$ over v'' for a given v' level of the upper state.

Table 5 displays the estimated radiative lifetimes of the upper electronic Λ−S states at $v' = 0$ only for several dipole allowed transitions. Our calculations suggest that $1^1\Sigma^+-4^1\Sigma^+$ is the strongest possible transition with the shortest partial lifetime, although it is not experimentally observed so far. The second allowed transition from the $4^1\Sigma^+$ state, namely, $2^1\Sigma^+-4^1\Sigma^+$, has also large transition probability. The partial lifetime of the experimentally observed transition $X^3\Sigma^--A^3\Pi$ is about 456 ns. However, this estimation does not take into account of the spin−orbit interaction. The total lifetime of the $4^1\Sigma^+$ state at $v' = 0$ is found to be 43 ns, which is the shortest-lived state among

TABLE 6: Radiative Lifetimes of the $A^3\Pi_{0^+}$ State of GaAs

	lifetimes of the $A^3\Pi_{0^+}$ state (μs)		
transition	$v' = 0$	$v' = 1$	$v' = 2$
$X^3\Sigma^-_{0^+} \leftarrow A^3\Pi_{0^+}$	69.4	73.5	72.6
$1^3\Pi_{0^+} \leftarrow A^3\Pi_{0^+}$	10.7	8.1	7.2
$2^1\Sigma^+_{0^+} \leftarrow A^3\Pi_{0^+}$	1.5×10^4	3.5×10^3	3.3×10^3
$1^1\Sigma^+_{0^+} \leftarrow A^3\Pi_{0^+}$	1.1×10^4	1.5×10^4	2.3×10^4
$X^3\Sigma^-_1 \leftarrow A^3\Pi_{0^+}$	1.2	1.3	1.7
$1^3\Pi_1 \leftarrow A^3\Pi_{0^+}$	83.7	76.2	64.2
$1^1\Pi_1 \leftarrow A^3\Pi_{0^+}$	1.9×10^3	2.0×10^3	1.6×10^3
total lifetimes			
τ ($A^3\Pi_{0^+}$)	1.05	1.09	1.32

all. The observed $A^3\Pi$ state has a lifetime of about 440 ns, when no spin−orbit coupling is considered. In Table 6 we have given the radiative lifetimes of the 0^+ component of $A^3\Pi$ for three vibrational levels $v' = 0$, 1, and 2. As per observation of Lemire et al.,[6] other components of $A^3\Pi$ with $\Omega = 2$, 1, 0^- undergo predissociation. Summing up the transition probabilities of seven possible transitions from the $A^3\Pi_{0^+}$ component (four 0^+-0^+ ($\Delta\Omega = 0$) and three $1-0^+$ ($\Delta\Omega = \pm 1$)), the total lifetime estimated for the $A^3\Pi_{0^+}$ state at $v' = 0$ is about 1050 ns and it increases with the increase in v'. The value is somewhat larger than the observed one which fluctuates widely between 600 and 10 ns.

Comparison with Other Calculations. Several calculations on the neutral GaAs molecule and its ions $GaAs^+$ and $GaAs^-$ have been performed by Balasubramanian.[14] These authors have computed spectroscopic constants and potential energy curves of Λ−S states up to the energy of 25 000 cm^{-1} by the complete active space MCSCF (CASSCF) followed by first-order CI (FOCI) and second-order CI (SOCI) calculations. Table 2 shows the comparison of the CASSCF/SOCI spectroscopic constants with our values. In general, r_e values calculated in this paper are somewhat larger, while the vibrational frequencies and the transition energies are smaller than Balasubramanian's results. Three quintet states have been calculated by Balasubramanian using the CASSCF/FOCI method. We have not studied $^5\Pi$ (III) which lies above 50 000 cm^{-1}. However, some other strongly bound states such as $4^1\Sigma^+$, $1^5\Sigma^+$, and $2^5\Sigma^+$ lying below 50 000 cm^{-1} are not studied before. Large discrepancies may be noted for r_e and ω_e values of $2^1\Sigma^+$ and $2^3\Sigma^+$ states. The strong avoided crossing in the potential energy curve of the $2^3\Sigma^+$ state is not shown in ref 14. The state which undergoes a sharp avoided crossing with a shallow potential energy curve of $3^1\Sigma^+$ is also not calculated in the work of Balasubramanian. Meier et al.[15] have studied several excited states of GaAs by MRD-CI study. Three excited $^3\Pi$ states are calculated by these authors. The $2^3\Pi$ state has been found to lie at 17 700 cm^{-1} compared with our T_e values of 16 832 cm^{-1}. The bond length is comparable, while the vibrational frequency is larger than our value by 6 cm^{-1}. Spectroscopic features of all important $A^3\Pi$ state studied by Meier et al.[15] matches well with the present study with the exception of ω_e. None of the previous calculations has included the spin−orbit coupling. Therefore, the present work reports for the first time the effects of the spin−orbit interaction. The predissociation of $A^3\Pi_{0^-}$, $A^3\Pi_1$, and $A^3\Pi_2$ states through the coupling with the components of the repulsive $1^5\Sigma^-$ state observed by Lemire et al.[6] has also been suggested by Balasubramanian[14] and Meier et al.[15] The fact that the $A^3\Pi_{0^+}$ component survives the predissociation has been nicely demonstrated in the potential energy curves of the Ω-states computed here.

IV. Conclusion

MRDCI calculations of the GaAs molecule based on RECPs in which 3d, 4s, and 4p electrons are kept in the valence space confirm the ground state as $X^3\Sigma^-$. There are at least 17 bound Λ−S states within 45 000 cm^{-1} of energy. Spectroscopic parameters of the ground and third $^3\Pi$ states designated as $X^3\Sigma^-$ and $A^3\Pi$, respectively, which are observed in the resonant two photon ionization spectroscopy by Lemire et al.[6] compare well with our calculated results. The vibrational frequencies of some of the states of GaAs are found to be lower than the other available experimental or calculated data. The present calculations suggest that the splitting of the two spin−orbit components of the $X^3\Sigma^-$ state is about 76 cm^{-1} with $X^3\Sigma^-_{0^+}$ being the ground state. This is in contrary to the experimental findings of Lemire et al.[6] according to which the ground state is $X^3\Sigma^-_1$, and the corresponding 0^+ component is 43 cm^{-1} above it.

Potential energy curves of four Ω-components of the $A^3\Pi$ state confirm the observed predissociation of the $A^3\Pi_2$, $A^3\Pi_1$, and $A^3\Pi_{0^-}$ states through the interaction with the corresponding components of the repulsive $1^5\Sigma^-$ state. The $A^3\Pi_{0^+}$ state survives from the predissociation. The calculated transition energy of $A^3\Pi_{0^+}$ is about 22 178 cm^{-1} compared with the experimental value of 23 568 cm^{-1}. The r_e value estimated in this calculation is 0.095 Å higher than the observed value of 2.662 Å, while the equilibrium vibrational frequency is lower than the experimental value by about 27 cm^{-1}. Transition probabilities calculated from the CI wave functions show that the transition from the excited $4^1\Sigma^+$ state to the lowest state of the same symmetry is the strongest among all. The $X^3\Sigma^- - A^3\Pi$ transition which is the only observed transition is also reasonably strong. The radiative lifetime of the $A^3\Pi$ state at $v' = 0$ is found to be 440 ns. The present calculations reveal that the total lifetimes of the $A^3\Pi_{0^+}$ component at the lower vibrational levels $v' = 0$, 1, and 2 are 1050, 1090, and 1320 ns, respectively, as compared with the observed values in the range 10−600 ns.

Acknowledgment. The authors thank Prof. R. J. Buenker, Wuppertal, Germany for giving us the permission to use his MRDCI codes. The financial support from the CSIR, India under the Grant 01(1427)/96/EMR-II is gratefully acknowledged.

References and Notes

(1) O'Brien, S. C.; Liu, Y.; Zhang, Q.; Heath, J. R.; Tittel, F. K.; Curl, R. F.; Smalley, R. E. *J. Chem. Phys.* **1986**, *84*, 4074.
(2) Liu, Y.; Zhang, Q.; Tittel, F. K.; Curl, R. F.; Smalley, R. E. *J. Chem. Phys.* **1986**, *85*, 7434.
(3) Zhang, Q.; Liu, Y.; Curl, R. F.; Tittel, F. K.; Smalley, R. E. *J. Chem. Phys.* **1988**, *88*, 1670.
(4) Wang, L.; Chibante, L. P. F.; Tittel, F. K.; Curl, R. F.; Smalley, R. E. *Chem. Phys. Lett.* **1990**, *172*, 335.
(5) Jin, C.; Taylor, K.; Conciecao, J.; Smalley, R. E. *Chem. Phys. Lett.* **1990**, *175*, 17.
(6) Lemire, G. W.; Bishea, G. A.; Heidecke, S. A.; Morse, M. D. *J. Chem. Phys.* **1990**, *92*, 121.
(7) Van Zee, R. J.; Li, S.; Weltner, W., Jr. *J. Chem. Phys.* **1993**, *98*, 4335.
(8) Knight, L. B. Jr.; Petty, J. T. *J. Chem. Phys.* **1988**, *88*, 481.
(9) Stwarts, C. A.; McGill, T. C.; Goddard III, W. A. *Surf. Sci.* **1981**, *110*, 400.
(10) Stwarts, C. A.; Goddard III, W. A.; McGill, T. C. *J. Vac. Sci. Tₑchnol.* **1981**, *19*, 551.
(11) Lamfried, W. H.; Strehlow, R. *Phys. Status Solidi* **1982**, *B110*, K79.
(12) Balasubramanian, K. *J. Chem. Phys.* **1987**, *86*, 3410; Erratum: *J. Chem. Phys.* **1990**, *92*, 2123.
(13) Balasubramanian, K. *Chem. Rev.* **1990**, *90*, 93.
(14) Balasubramanian, K. *J. Mol. Spectrosc.* **1990**, *139*, 405.
(15) Meier, U.; Peyerimhoff, S. D.; Bruna, P. J.; Grein, F. *J. Mol. Spectrosc.* **1989**, *134*, 259.

(16) Lou, L.; Wang, L.; Chibante, L. P. F.; Laaksonen, R. T.; Nordlander, P.; Smalley, R. E. *J. Chem. Phys.* **1991**, *94*, 8015.
(17) Lou, L.; Nordlander, P.; Smalley, R. E. *J. Chem. Phys.* **1992**, *97*, 1858.
(18) Hurley, M. M.; Pacios, L. F.; Christiansen, P. A.; Ross, R. B.; Ermler, W. C. *J. Chem. Phys.* **1986**, *84*, 6840.
(19) Buenker R. J.; Peyerimhoff, S. D. *Theor. Chim. Acta* **1974**, *35*, 33.
(20) Buenker R. J.; Peyerimhoff, S. D. *Theor. Chim. Acta* **1975**, *39*, 217.
(21) Buenker, R. J. *Int. J. Quantum Chem.* **1986**, *29*, 435.
(22) Buenker, R. J.; Peyerimhoff, S. D.; Butcher, W. *Mol. Phys.* **1978**, *35*, 771.
(23) Buenker, R. J. In *Proceedings of the Workshop on Quantum Chemistry and Molecular Physics*; Burton, P., Ed.; University Wollongong: Wollongong, Australia; 1980; *Studies in Physical and Theoretical Chemistry*; Carbó, R., Ed.; Elsevier: Amsterdam, 1981; Vol. 21 (Current Aspects of Quantum Chemistry).
(24) Buenker, R. J.; Phillips, R. A. *J. Mol. Struct.* (THEOCHEM) **1985**, *123*, 291.
(25) Davidson, E. R. In *The World of Quantum Chemistry*; Daudel, R., Pullman, B., Ed.; Reidel: Dordrecht, 1974.
(26) Hirsch, G.; Bruna, P. J.; Peyerimhoff, S. D.; Buenker, R. J. *Chem. Phys. Lett.* **1977**, *52*, 442.
(27) Das, K. K.; Liebermann, H. P.; Buenker, R. J.; Hirsch, G. *J. Chem. Phys.* **1995**, *102*, 4518.
(28) Cooley, J. W. *Math. Comput.* **1961**, *15*, 363.
(29) Moore, C. E. *Atomic Energy Levels*; National Bureau of Standards: Washington, DC, 1971; Vol. 3.